

Continuous tuning of two-section, single-mode terahertz quantum-cascade lasers by fiber-coupled, near-infrared illumination

Cite as: AIP Advances 7, 055201 (2017); <https://doi.org/10.1063/1.4983030>

Submitted: 17 February 2017 • Accepted: 24 April 2017 • Published Online: 04 May 2017

 Martin Hempel,  Benjamin Röben,  Michael Niehle, et al.



View Online



Export Citation



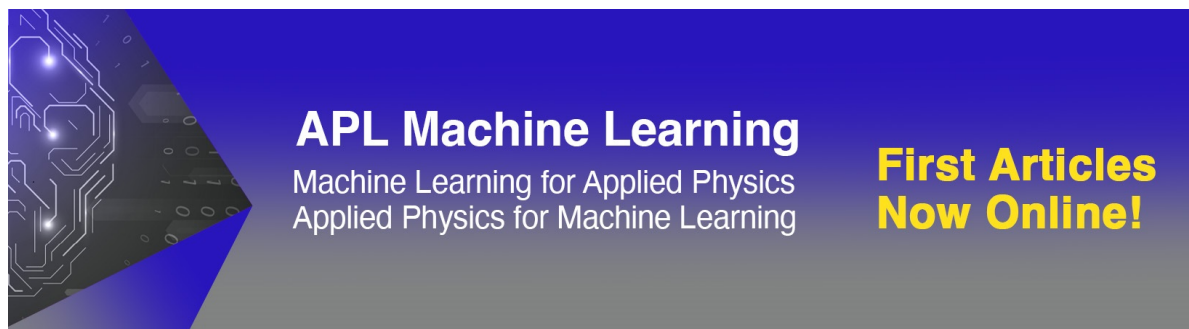
CrossMark

ARTICLES YOU MAY BE INTERESTED IN

[Fast continuous tuning of terahertz quantum-cascade lasers by rear-facet illumination](#)
Applied Physics Letters **108**, 191106 (2016); <https://doi.org/10.1063/1.4949528>

[Intrinsic frequency tuning of terahertz quantum-cascade lasers](#)
Journal of Applied Physics **123**, 213102 (2018); <https://doi.org/10.1063/1.5024480>

[Determination of the interface parameter in terahertz quantum-cascade laser structures based on transmission electron microscopy](#)
Applied Physics Letters **113**, 172101 (2018); <https://doi.org/10.1063/1.5042326>



APL Machine Learning
Machine Learning for Applied Physics
Applied Physics for Machine Learning

**First Articles
Now Online!**

Continuous tuning of two-section, single-mode terahertz quantum-cascade lasers by fiber-coupled, near-infrared illumination

Martin Hempel,^a Benjamin Röben, Michael Niehle, Lutz Schrottke, Achim Trampert, and Holger T. Grahn
Paul-Drude-Institut für Festkörperelektronik, Leibniz-Institut im Forschungsverbund Berlin e.V., Hausvogteiplatz 5–7, 10117 Berlin, Germany

(Received 17 February 2017; accepted 24 April 2017; published online 4 May 2017; publisher error corrected 9 May 2017)

The dynamical tuning due to rear facet illumination of single-mode, terahertz (THz) quantum-cascade lasers (QCLs) which employ distributed feedback gratings are compared to the tuning of single-mode QCLs based on two-section cavities. The THz QCLs under investigation emit in the range of 3 to 4.7 THz. The tuning is achieved by illuminating the rear facet of the QCL with a fiber-coupled light source emitting at 777 nm. Tuning ranges of 5.0 and 11.9 GHz under continuous-wave and pulsed operation, respectively, are demonstrated for a single-mode, two-section cavity QCL emitting at about 3.1 THz, which exhibits a side-mode suppression ratio better than -25 dB. © 2017 Author(s). All article content, except where otherwise noted, is licensed under a Creative Commons Attribution (CC BY) license (<http://creativecommons.org/licenses/by/4.0/>). [<http://dx.doi.org/10.1063/1.4983030>]

Frequency tuning is an important prerequisite for state-of-the-art spectroscopy. It allows for the adjustment of the emission frequency over a certain range, e.g., for modulation spectroscopy techniques.^{1–3} In addition to intrinsic frequency tuning mechanisms for terahertz (THz) quantum-cascade lasers (QCLs) via current and temperature change, additional concepts have been tested during the last decade. Among them are external cavity setups,^{4,5} mechanically tuned cavities,^{6–8} coupled cavities,^{9,10} material condensation,^{11,12} and three-terminal configurations.¹³ However, most of these approaches rely on very sophisticated external or built-in structures, are optimized for a certain lasing wavelength and active material, or exhibit a very limited tuning range. Recently, a fast and continuous tuning of multi-mode terahertz (THz) quantum-cascade lasers (QCLs), independent of a specific active region design, has been demonstrated by illuminating their rear facets with a near-infrared diode laser.¹⁴ These THz QCLs are based on single-plasmon waveguides, and the frequency tuning was attributed to a change of the optical length of the Fabry-Pérot cavity.¹⁴ THz QCLs with Fabry-Pérot resonators typically operate in the multi-mode regime, but for a variety of spectroscopic applications, e.g., in heterodyne detection schemes,^{15–19} single-mode operation is desired. There are two common concepts to achieve a reliable single-mode operation: (i) the application of a distributed feedback (DFB) grating to the cavity,^{20–22} and (ii) a two-section cavity, where the allowed modes are determined by the lengths of the two sub-cavities.^{23–25} In this letter, we will compare the frequency tuning behavior of both concepts using a fiber optics-based, near-infrared light illumination scheme.

Based on the illumination arrangement presented in Ref. 14, we have improved the illumination of the rear facet of the THz QCL using a diode laser (DL) by coupling the light through an optical fiber instead of mounting the DL on the THz QCL submount. This has three advantages: (i) the excess heat of the DL is kept outside the cryocooler necessary to operate the THz QCL so that the cooler can maintain lower temperatures; (ii) while keeping the fiber in place, the THz QCL can be changed quite easily, which is not the case when the DL is soldered on the QCL submount; (iii) the illumination beam geometry is much more flexible.

^ahempel@pdi-berlin.de

The DL (DILAS I2F2S22-775.10-2C-SS14) emits at 777 nm with a lasing threshold at 600 mA and a slope efficiency of 1.14 W/A. The maximal continuous-wave (cw) output power is 3 W at 3,500 mA. The DL is coupled to a 1-m-long, 200- μm core-diameter multi-mode fiber (ThorLabs FG200LCC) with a numerical aperture of 0.22 via an SMA connector at the DL module. The DL is driven by a cw current source (ILX LDX-3232). The bare and flat-cleaved fiber end is aligned to illuminate the rear facet of the THz QCL as shown in Fig. 1(a).

For the investigation of the tuning behavior of DFB QCLs, three QCLs were used with different active regions emitting at about 3.1, 3.5, and 4.7 THz with lateral DFB grating periods of 12.8, 12.8, and 8.52 μm , respectively.²² All QCLs are 0.12 mm wide, while their lengths vary from 1.31 mm to 2.23 mm to 2.47 mm for the 3.1, 3.5, and 4.7 THz QCLs, respectively. For pulsed operation, we used an electrical pulse width of 500 ns and a repetition rate of 5 kHz. All three QCLs lase up to 85 K under short-pulse operation, delivering an output power of about 6.5 mW at 5 K heat sink temperature and a current density of 800 A/cm² in case of the 3.1 and 4.7 THz devices, while the 3.5 THz QCL emits about 5.3 mW at 5 K with 460 A/cm².

The two-section cavities were fabricated applying a method already successfully employed for near-infrared DLs, mid-infrared QCLs, and THz QCLs.^{23–25} The QCL laser cavity is separated into two parts by focused-ion beam (FIB) processing of an already mounted and characterized QCL, which lases in cw operation at about 3.1 THz up to temperatures of 73 K emitting about 10 mW for 400 A/cm² at 10 K. The employed FIB system (JEOL IB4501 dual-beam microscope) uses a focused Ga ion beam with an acceleration voltage of 30 kV. The FIB cut has a length of 145 μm , a width of 8 μm , and a depth of 14 μm , preventing an electrical short cut by burying the used Ga ions in the semi-insulating substrate under the 11- μm -thick epitaxial layer. The 120- μm -wide emitter stripe was divided into an 810- μm - and a 240- μm -long section. A schematic and an electron microscopy image of the cut are shown in Figs. 1(b) and 1(c), respectively.

The spectra are recorded with a high-resolution Fourier transform spectrometer (Bruker IFS 120HR) equipped with a 6- μm -thick broadband Mylar[®] beam splitter and a deuterated triglycine sulfate (DTGS) detector for the THz region. A spectral resolution of $\Delta\tilde{\nu} = 0.01 \text{ cm}^{-1}$ was used. The DL is always employed in cw operation, even when the QCL is used in pulsed operation, to avoid the influence of time-dependent additional heating.¹⁴

The results for the 3.5-THz DFB QCL are shown in Fig. 2(a). When the DL is off, the device exhibits single-mode operation at 3.526 THz (117.62 cm^{-1}). This mode shifts to higher frequencies reaching a maximal tuning range of 0.7 GHz at a diode laser current of $I_{\text{DL}} = 1,000 \text{ mA}$. However, starting from $I_{\text{DL}} = 750 \text{ mA}$ on, a second mode at about 3.540 THz (118.09 cm^{-1}) appears. While the intensity of the original mode decreases with increasing values of I_{DL} , the intensity of the new

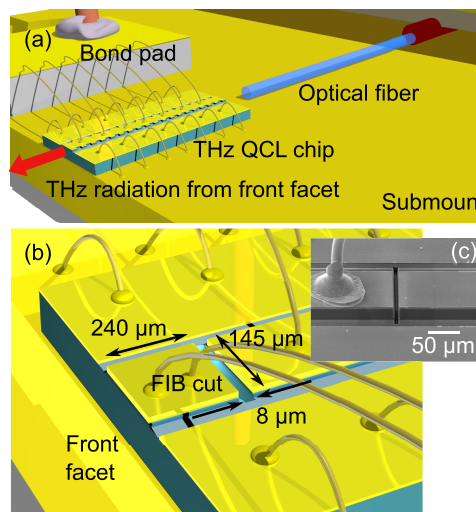


FIG. 1. (a) Schematic of the fiber-coupled DL illuminating the rear facet of the THz QCL. (b) Schematic of the FIB cut applied to the ridge of a THz QCL. (c) Electron microscopy image of the actual cut, seen from the side.

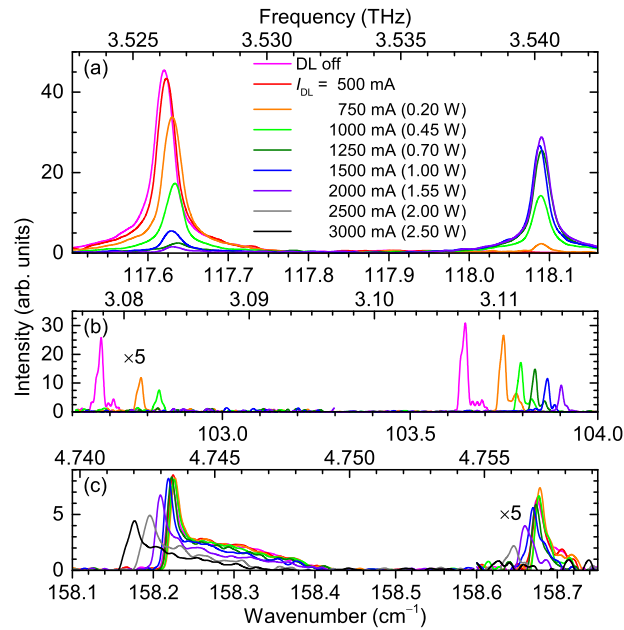


FIG. 2. (a) Spectrum of the 3.5-THz DFB QCL in pulsed operation with 500-ns pulses at a repetition rate of 5 kHz and a current of $I_{\text{QCL}} = 1,800$ mA. The heat sink temperature was set to 35 K. The DL is driven at different current values in cw operation. The DL optical power is indicated in brackets. (b) Spectra of the 3.1-THz DFB QCL with 500-ns pulses at 5 kHz and $I_{\text{QCL}} = 950$ mA at 35 K. (c) Spectra of the 4.7-THz DFB QCL with 500-ns pulses at 5 kHz and $I_{\text{QCL}} = 2,000$ mA at 45 K. The legend in (a) is also valid for (b) and (c).

mode increases. Therefore, this tuning scheme is not very effective for continuous tuning of a single mode when applied to a DFB THz QCL. In fact, it can be used to switch from one single mode to another one.

In order to verify that this result is independent of the actually used QCL, we repeated the experiment with two other DFB QCLs emitting at about 3.1 and 4.7 THz as shown in Figs. 2(b) and 2(c), respectively. Both devices exhibit lasing on two modes, one main mode and a side mode, when operated without DL illumination. With higher DL illumination powers, the modes exhibit a blue shift, similar to the case of the 3.5-THz QCL [cf. Fig. 2(a)]. In case of the 3.1-THz QCL in Fig. 2(b), the blue shift of the strongest mode covers 7.7 GHz, but with transfer of intensity to the side mode, while 1.5 GHz are achieved in case of the 4.7-THz QCL as shown in Fig. 2(c). In all investigated THz DFB QCLs, a transfer of the radiation intensity from the main to the side mode is present. Furthermore, DFB QCLs exhibiting two modes can be forced into single-mode operation by the illumination with the DL [cf. Fig. 2(b)]. The spectra in Figs. 2(b) and 2(c) appear to be asymmetrically broadened as an effect of cavity heating and finite widths of the leading and trailing edges of the current pulse. The influence of these effects, e.g., via cavity pulling,^{26,27} to the spectrum of the devices depends significantly on the design of the active region of the QCL. Therefore, the resulting spectral shapes are different for the devices investigated in Figs. 2(a)–2(c).

The mode switching of the DFB QCL under rear-facet illumination can be explained by the formation of a stop band, only allowing certain modes to propagate through the cavity.²⁰ Since this effect works along the entire length of the cavity, a frequency tuning mechanism acting only on a thin layer with a thickness of about $5 \mu\text{m}$ on the rear facet is not expected to compete with the DFB mode selection mechanism. However, it is well known that the exact phase matching of the DFB grating on the facet plays an important role for the selection of the Fabry-Pérot mode, which is in competition with the DFB mode.^{22,28,29} The transfer of output power from one spectral mode to another induced by the DL illumination is the result of such competition, since the DL illumination results in a small change of the Fabry-Pérot cavity length and therefore the spectral position of the cavity mode.

For the two-section cavity device, Fig. 3(a) shows the spectra of the original QCL and Fig. 3(b) of the QCL after it has been cut by FIB for various currents I_{QCL} with the QCL employed in pulsed

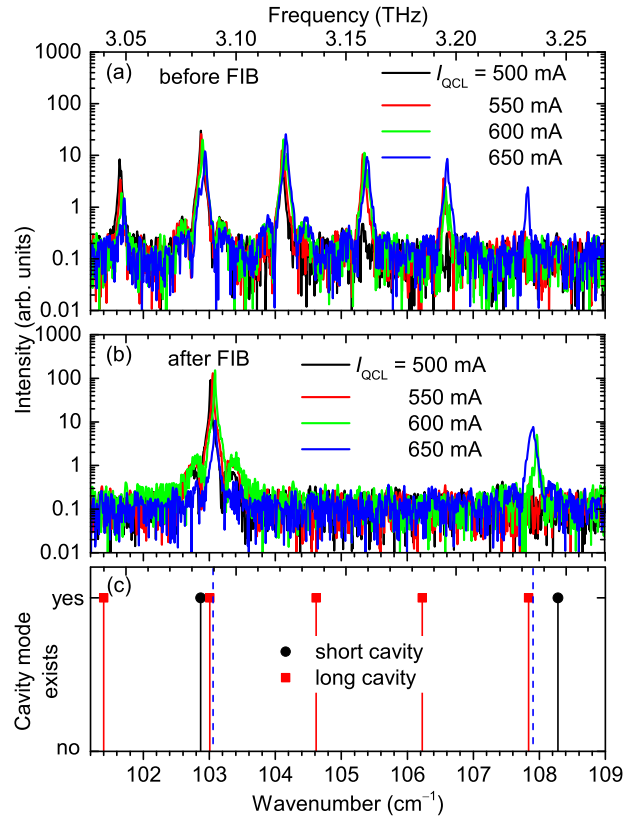


FIG. 3. (a) Lasing spectra of the original QCL before applying the FIB cut at different current levels in pulsed operation with 500-ns pulses at a repetition rate of 5 kHz for 35 K heat sink temperature. (b) Lasing spectra after applying the FIB cut, using the same operating parameters as in (a). (c) Calculated position of the cavity modes with refractive group index of 3.84 for the long and short section of the cavity (solid lines). The dashed lines indicate the position of the modes observed in the experiment.

operation at 35 K. The original QCL exhibits 5 to 6 spectral modes, while after the FIB cut only one prominent mode at about 3.09 THz and, for elevated currents above $I_{QCL} = 550$ mA, a second weaker mode at 3.23 THz appear.

The single-mode operation of the two-section cavity laser can be modeled by calculating the Fabry-Pérot modes of the two individual cavities. For the two-section QCL, only modes are allowed which exist in both cavities at almost identical frequencies.²⁵ The calculated modes for the two sections of the QCL are displayed in Fig. 3(c). An effective refractive group index for the QCL cavity of 3.84 was determined from the spacing of the Fabry-Pérot modes of the original QCL and the measured cavity length. As discussed in Ref. 25, this simplified calculation compared to the fully coupled-mode cavity model²⁸ is only feasible if the modes in the sub-cavities are sufficiently strong. In order to achieve this, the FIB cut has to act as a semi-transparent mirror with sufficiently high reflectivity to form two cavities. It is surprising that, in case of the long wavelength of about 100 μm in vacuum of the used THz QCL, an only 8- μm -wide gap in the cavity is sufficient to fulfill this condition. It indicates the significance of creating two new intra-cavity facets rather than of the gap between the cavity sections. A likely reason for this is the effect of field enhancement at the metal edges, which were introduced by cutting the upper gold contact by the FIB processing.³⁰

In pulsed operation, the two modes of the short and long cavity at 3.09 and 3.24 THz are sufficiently close together to contribute to lasing in the combined system [cf. Fig. 3(b)]. For cw operation, the QCL only emits the mode at 3.09 THz. A lower limit for the side mode suppression ratio (SSR) can be estimated by considering the maxima of the noise level in comparison to the lowest-intensity lasing mode. We end up with an SSR better than -25 dB for both pulsed (up to $I_{DL} = 550$ mA) and cw operation. Furthermore, the output power of all modes in multi-mode operation before the FIB cut is transferred into one mode during single-mode operation [cf. Figs. 3(a) and 3(b)]. The application

of the FIB cut to an already characterized laser has the advantage to select a certain frequency within the gain region of the laser by choosing a particular position of the FIB cut. Especially, the effective refractive group index can be determined from the multi-mode spectrum of the original QCL.

By independently varying the currents applied to the two sections of the QCL (not shown here), we can already achieve a tuning range of about 2.5 GHz. In order to enhance the tuning range, we applied the fiber coupling to the rear facet of the longer cavity part. For these experiments, both sections were electrically connected in parallel, and the current was set to $I_{\text{QCL}} = 500$ mA for pulsed operation. Therefore, we only use the frequency side mode suppression and no tuning by varying independently the current values for both QCL cavities. The distance between the fiber tip and the rear facet is $940 \mu\text{m}$. Using a small angle of 18° with respect to normal incidence prevents back-reflected, near-infrared light to re-enter the optical fiber.

Figure 4(a) shows the spectra under pulsed operation with increasing DL illumination power. Due to the dynamic variation of the temperature and current in pulsed operation, the spectral peaks are broadened, and the line shape becomes much more complex. According to additional measurements, which are not shown, a heating-up of the device causes a red-shift.³ However, the increase of the DL illumination power clearly results in a blue shift of the lasing frequency as shown in Fig. 4(a). Below the DL threshold current of $I_{\text{DL,th}} = 600$ mA, the radiation of the DL is due to electroluminescence, which is in the mW-range as compared to several hundreds of mW above $I_{\text{DL,th}}$. The corresponding frequency shift is very small. The largest frequency tuning range is achieved at the highest possible DL power. A further blue shift is expected for even larger illumination powers, but the application of these powers is limited by the damage threshold of the rear facet due to the heating or by the limited cooling capacity of the used cryocooler.

For high-resolution spectroscopy, the QCL and the DL have to be used in cw operation so that both lasers are in thermal equilibrium with the heat sink. Then, their frequencies become stable, and the QCL line width is much narrower. Figure 4(b) shows the results of the QCL under cw operation for various DL driving currents. A clear blue shift of the QCL frequency is visible above $I_{\text{DL,th}}$, while below $I_{\text{DL,th}}$ a very small red shift takes place. The maximally applied DL power is under cw operation limited by the cooling capacity of the cryocooler, since the absorbed near-infrared radiation at the QCL rear facet causes an additional heating. Over the entire tuning range, the device maintains single-mode operation.

Figure 4(c) shows the peak position of the lasing modes for pulsed and cw operation extracted from Figs. 4(a) and 4(b), respectively. The maximal tuning range in single-mode operation of the

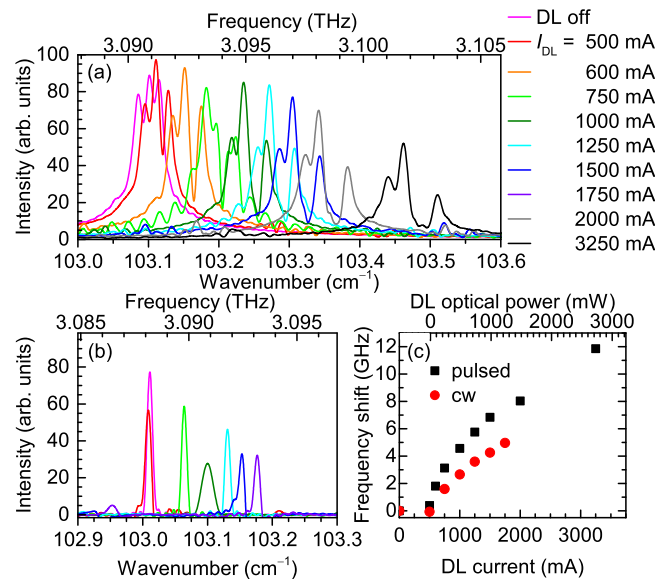


FIG. 4. (a) Frequency tuning of the two-section QCL for pulsed operation at 500 mA and 45 K for different DL driving currents. (b) Frequency tuning for the same QCL as in (a) under cw operation at 450 mA and 50 K for different DL driving currents. The legend in (a) is also valid for (b). (c) Frequency shift extracted from the peak positions in (a) and (b).

THz QCL achieved at 2.70 W DL optical power during pulsed operation of the QCL is 11.9 GHz. A maximal tuning range of 5.0 GHz can be achieved for cw operation. While the maximal tuning range in the pulsed case was limited by the maximal optical power of the DL system, the cw tuning range was limited by the cooling capacity of the cryocooler. Moreover, the heat sink temperature itself has a negligible effect on the tuning range as discussed in Ref. 14. Therefore, we chose slightly different heat sink temperatures for pulsed and cw operation in order to achieve an optimized and adapted performance of the cryocooler.

In conclusion, a fiber-coupled DL illumination scheme was used for frequency tuning of THz QCLs. We have shown that the illumination-induced tuning can result in a mode switching in DFB QCLs. Moreover, a two-section cavity device was produced in a post-processing step using FIB starting with an already characterized QCL. This two-section, coupled-cavity THz QCL allows to combine the advantages of the illumination-induced tuning with single-mode operation. The presented 3.1-THz two-section QCL provided an SSR of better than -25 dB. Under pulsed operation, the maximal frequency tuning range is 11.9 GHz, while for cw operation the tuning range amounts to 5 GHz.

We would like to thank W. Anders, K. Biermann, and M. Hörcke for sample preparation, A. Tahraoui for fruitful discussions, and T. Flissikowski for a careful reading of the manuscript. Part of this work was supported by the Deutsche Forschungsgemeinschaft.

- ¹ M. A. Kramer, R. W. Boyd, L. W. Hillman, and C. R. Stroud, *J. Opt. Soc. Am. B* **2**, 1444 (1985).
- ² R. Eichholz, H. Richter, M. Wienold, L. Schrottke, R. Hey, H. T. Grahn, and H.-W. Hübers, *Opt. Express* **21**, 32199 (2013).
- ³ H. Richter, M. Wienold, L. Schrottke, K. Biermann, H. T. Grahn, and H.-W. Hübers, *IEEE Trans. Terahertz Sci. Technol.* **5**, 539 (2015).
- ⁴ J. Xu, J. M. Hensley, D. B. Fenner, R. P. Green, L. Mahler, A. Tredicucci, M. G. Allen, F. Beltram, H. E. Beere, and D. A. Ritchie, *Appl. Phys. Lett.* **91**, 121104 (2007).
- ⁵ A. W. M. Lee, B. S. Williams, S. Kumar, Q. Hu, and J. L. Reno, *Opt. Lett.* **35**, 910 (2010).
- ⁶ Q. Qin, B. S. Williams, S. Kumar, J. L. Reno, and Q. Hu, *Nature Photon.* **3**, 732 (2009).
- ⁷ L. Mahler, A. Tredicucci, F. Beltram, H. E. Beere, and D. A. Ritchie, *Opt. Express* **18**, 19185 (2010).
- ⁸ Q. Qin, J. L. Reno, and Q. Hu, *Opt. Lett.* **36**, 692 (2011).
- ⁹ I. Kundu, P. Dean, A. Valavanis, L. Chen, L. Li, J. E. Cunningham, E. H. Linfield, and A. G. Davies, *Opt. Express* **22**, 16595 (2014).
- ¹⁰ D. Turčinková, M. I. Amanti, G. Scalari, M. Beck, and J. Faist, *Appl. Phys. Lett.* **106**, 131107 (2015).
- ¹¹ A. Benz, C. Deutsch, M. Brandstetter, A. M. Andrews, P. Klang, H. Detz, W. Schrenk, G. Strasser, and K. Unterrainer, *Sensors* **11**, 6003 (2011).
- ¹² D. Turčinková, M. I. Amanti, F. Castellano, M. Beck, and J. Faist, *Appl. Phys. Lett.* **102**, 181113 (2013).
- ¹³ K. Ohtani, M. Beck, and J. Faist, *Appl. Phys. Lett.* **104**, 011107 (2014).
- ¹⁴ M. Hempel, B. Röben, L. Schrottke, H.-W. Hübers, and H. T. Grahn, *Appl. Phys. Lett.* **108**, 191106 (2016).
- ¹⁵ H. W. Hübers, S. G. Pavlov, A. D. Semenov, R. Köhler, L. Mahler, A. Tredicucci, H. E. Beere, D. A. Ritchie, and E. H. Linfield, *Opt. Express* **13**, 5890 (2005).
- ¹⁶ M. Lee, M. C. Wanke, M. Lerttamrab, E. W. Young, A. D. Grine, J. L. Reno, P. H. Siegel, and R. J. Dengler, *IEEE J. Sel. Top. Quantum Electron.* **14**, 370 (2008).
- ¹⁷ H. Richter, A. D. Semenov, S. G. Pavlov, L. Mahler, A. Tredicucci, H. E. Beere, D. A. Ritchie, K. S. Il'in, M. Siegel, and H.-W. Hübers, *Appl. Phys. Lett.* **93**, 141108 (2008).
- ¹⁸ P. Khosropanah, W. Zhang, J. N. Hovenier, J. R. Gao, T. M. Klapwijk, M. I. Amanti, G. Scalari, and J. Faist, *J. Appl. Phys.* **104**, 113106 (2008).
- ¹⁹ Y. Ren, J. N. Hovenier, R. Higgins, J. R. Gao, T. M. Klapwijk, S. C. Shi, B. Klein, T.-Y. Kao, Q. Hu, and J. L. Reno, *Appl. Phys. Lett.* **98**, 231109 (2011).
- ²⁰ H. Kogelnik and C. V. Shank, *J. Appl. Phys.* **43**, 2327 (1972).
- ²¹ S. O'Brien and E. P. O'Reilly, *Appl. Phys. Lett.* **86**, 201101 (2005).
- ²² M. Wienold, A. Tahraoui, L. Schrottke, R. Sharma, X. Lü, K. Biermann, R. Hey, and H. T. Grahn, *Opt. Express* **20**, 11207 (2012).
- ²³ L. A. Coldren, B. I. Miller, K. Iga, and J. A. Rentschler, *Appl. Phys. Lett.* **38**, 315 (1981).
- ²⁴ H. Li, J. M. Manceau, A. Andronico, V. Jagtap, C. Sirtori, L. H. Li, E. H. Linfield, A. G. Davies, and S. Barbieri, *Appl. Phys. Lett.* **104**, 241102 (2014).
- ²⁵ K. Pierściński, D. Pierścińska, M. Pluska, P. Gutowski, I. Sankowska, P. Karbownik, A. Czerwinski, and M. Bugajski, *J. Appl. Phys.* **118**, 133103 (2015).
- ²⁶ L. A. Dunbar, R. Houdré, G. Scalari, L. Sirigu, M. Giovannini, and J. Faist, *Appl. Phys. Lett.* **90**, 141114 (2007).
- ²⁷ H. Zhang, G. Scalari, J. Faist, L. A. Dunbar, and R. Houdré, *J. Appl. Phys.* **108**, 093104 (2010).
- ²⁸ H. A. Haus and W. Huang, *Proc. IEEE* **79**, 1505 (1991).
- ²⁹ A. Laakso, M. Dumitrescu, J. Viheriälä, J. Karinen, M. Suominen, and M. Pessa, *Opt. Quantum Electron.* **40**, 907 (2008).
- ³⁰ S. Kohen, B. S. Williams, and Q. Hu, *J. Appl. Phys.* **97**, 053106 (2005).